ICAS 2021 SHANG HAI
International Council of the Aeronautical Sciences
32nd Congress of the International Council of the Aeronautical Sciences
September 6-10, 2021 Pudong Shangri-La, Shanghai, China

NUMERICAL STUDY OF DITCHING CHARACTERISTICS OF BWB AIRCRAFT

Shili Ding[1], Qiulin Qu[1], Peiqing Liu[1,#]

[1]Key Laboratory of Fluid Mechanics (Beihang University), Ministry of Education, Beijing 100191, People's Republic of China

[#]e-mail: lpq@buaa.edu.cn

Abstract

In this paper, the skipping motion of a blended wing body (BWB) aircraft during ditching is investigated numerically using the Star-CCM+ solver. Based on the finite volume method (FVM), the volume-of-fluid model and the dynamic overset mesh method are selected to simulate the interaction of the aircraft and waves. During ditching with the high horizontal speed as well as the low pitch attitude, the blended wing body aircraft skips on the water. The results show that the horizontal speed plays a significant role in the skipping motion. And the change of pitch angle is always accompanied by the skipping motion of the blended wing body aircraft. For the influence of wavy environment, the wave surface mainly affects the moving amplitude and the speed deceleration of the BWB aircraft.

Keywords: ditching, overset mesh, blended wing body aircraft.

1. Introduction

Ditching is a significant part of the aircraft airworthiness certification. As a promising development direction of passenger aircrafts, the blended wing body aircraft due to its flat bottom structure will result in different motion characteristics from the conventional passenger aircraft during ditching, especially on the wavy water surface. Russia's Central Institute of Fluid Mechanics (ЦАГИ) divides ditching into "planned" and "unplanned"[1]. The former refers to a planned and controlled ditching due to fuel exhaustion or engine shutdown. And the latter means that some unexpected situations could cause ditching behaviors during the take-off and landing process of aircraft, which is more dangerous than the former. The planned ditching is regarded as a relatively safe ditching behavior under ideal conditions. In actual situations, however, considering the experience of pilot's driving and the complexity of the ditching environment, it is difficult for the pilot to achieve the expected motion parameters of the aircraft during the ditching procedure[2]. The behaviors and mechanical characteristics of ditching of blended wing body aircraft are investigated in this paper, where the BWB aircraft loses its power as well as attitude control with high horizontal speed.

The blended wing body aircraft[3], resembling the flying wing, is a tailless airplane design for future air transportation that integrates the fuselage and the wing. This technique is applied in many types of aircrafts, including the B-2 stealth bomber, BWB-450[4], SAX-40[5], and so on. Due to the flat body shape and the larger wing area, the BWB aircraft may appear more violent pitch and heave motions, such as porpoising and skipping[6]. Therefore, it is very necessary to investigate the mechanical performance of ditching of the blended wing body aircraft, especially in the rough wavy environment. The motions of porpoising and skipping belong to dynamic longitudinal instability, which come from seaplane performances in period of landing or taking off from water[7]. These dangerous behaviors could result in serious damage to the aircraft structure. As shown in Figure 1, porpoising is an undulating motion about pitch and heave with some part of the aircraft always in contact with the water. While if the aircraft gets into the ditching state with higher horizontal speed and lower attitude, it could behave undesirably such as skipping. Either skipping or porpoising appears in the primary stage of ditching. As the horizontal speed of aircraft continues to decrease, the aircraft gets into the stage of planning, where both pitch and heave motion are no longer obvious. Eventually, the horizontal speed reduces to zero and the aircraft is floating on the water.

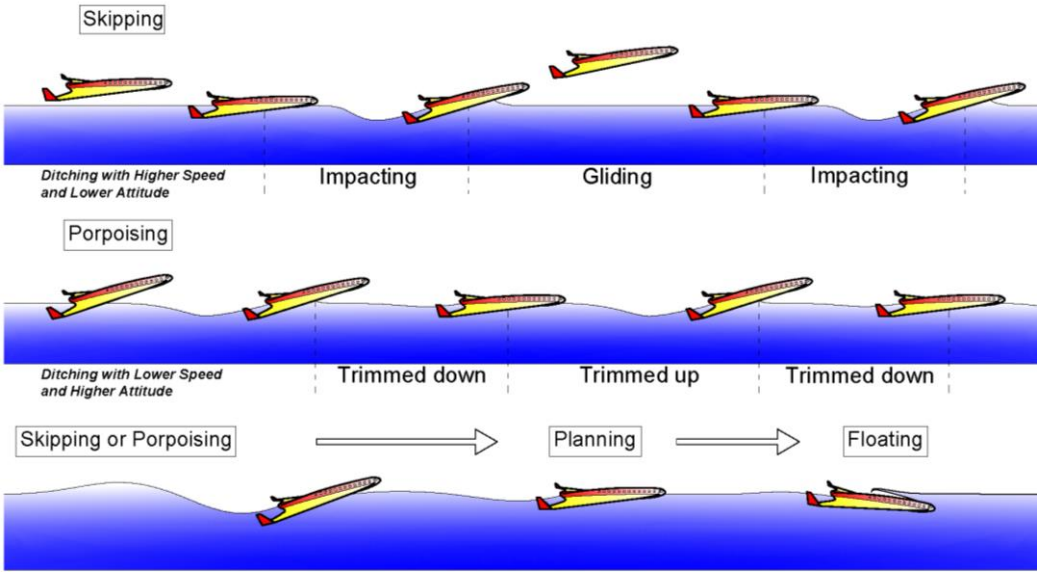

Figure 1 – Ditching procedure of a BWB aircraft.

Preliminary researches on the safety of aircraft ditching can be traced back to Word Wall II, when ditching characteristics of different aircrafts were mainly investigated via lots of tests and experiments, including towed model test, controlled launching model test, free launching test, full-scale drop test and full-scale ditching test. Among the test studies in various countries, the model tests conducted in the Towing Tanks No. 1 and No. 2 from the NACA Langley Laboratory in the United States are the most comprehensive. In 1943, Jhon B. Parkinson[10] obtained the motion characteristics of skipping of seaplane through experiments and explained that the poor ventilation from the shallow step of seaplane leads to skipping on the water. From 1940 to 1975, Lloyd J. Fisher[11] and others did substantial ditching tests on scaled aircraft models, manifesting that flattened cross sections in combination with high longitudinal curvature tend to tend to cause skipping. These tests indicate that during ditching on the water, the swept-wing fighter (F7U-3[9]) and the flying-wing bomber (Northrop B-35[6]) will also exhibit unstable movements of porpoising and skipping. In 1987, Darrol Stinton[7] further compared the difference between porpoising and skipping and illustrated that porpoising at higher speeds results in skipping. The above experimental researches also show that the skipping motion of seaplane or blended wing body aircraft at high horizontal speeds and low attitude is more likely to cause more uncertain dangers to aircrafts. Although numerous tests of aircraft models offer the relatively complete movement process of ditching behavior from the first contact with water to floating, it is such experiments that perform difficulty in describing the local load of aircraft in detail as well as costly.

Benefiting from the development of computational efficiency and numerical calculation methods, the researches of ditching of aircraft based on numerical methods get gradually matured, such as boundary element method (BEM), finite element method (FEM), smoothed particle hydrodynamics method (SPH) and finite volume method (FVM). These methods make it possible to reveal the details of local flow. Among these methods, the finite volume method combining with volume of fluid (VOF) method has become a relatively common method for the numerical simulation of aircraft ditching, of which advantage is to simulate accurately the local load and free surface. It is convenient to analyze and display the mechanical characteristics of the aircraft including the tail suction phenomenon in the process of ditching of aircraft.

For the researches of the conventional tube and wing aircraft design, in 2007, Streckwall and Lindnau[12] used the program DITCH based on the momentum method and the solver Comet based on VOF method to simulate the water impact procedure of fuselages with various rear shapes. In 2015, Qu[13] and others applied the global moving mesh (GMM) method to numerically simulate the ditching process of NACA TN 2929 model, which was compared with experimental data to show great simulation accuracy.

Compared with the traditional layout of the tube fuselage and wings, the blended wing body aircraft has a flatter fuselage and a relatively smooth transition of fuselage and wing, which makes higher

lift-to-drag ratio and greater passenger capacity. Meanwhile, the BWB aircraft should withstand more severe hydrodynamic impact during ditching. In 2017, Ralf Sturm and Martin Hepperle of German Aerospace (DLR)[14] evaluated the crashworthiness of the model of the NACRE blended wing body aircraft based on the SPH method and the FEM method at the beginning of ditching. Their research demonstrates that the blended wing body aircraft exhibits a more robust crash behavior during ditching procedure than conventional aircraft. Nevertheless, the simulation fails to last so long that the changing trend of movement could be revealed in their study.

Overset mesh method is a dynamic grid strategy which achieves the transfer of numerical information between different grid computational domains by interpolation calculation of grid cells. Without mesh reconstruction and mesh deformation, overset mesh method avoids poor quality grids generating. In 2016, Zhirong Shen[15] and others applied overset mesh to numerically simulate the green water impact force and breakwater areas on ships, where they indicated that the dynamic overset grid technique show greater flexibility for simulating large-amplitude motions. In 2018, Dominic DJ Chandar[16] and others compared the performances of overset mesh technique in OPERA based on open source code OpenFOAM, ANSYS Fluent and Star-CCM+, which proclaims that Star-CCM+ solver behaves superior to others in terms of interpolation method and robustness.

This paper selects Liebeck's BWB-450[4] aircraft model with the initial ditching parameters in reference[14] to simulate the ditching process on calm water and wavy water respectively, in order to investigate the behavior trend of blended wing body aircraft as well as its mechanical characteristics.

2. Numerical Method

The commercial computational fluid dynamics solver Star-CCM+ 12.02 is employed in this paper. The finite volume method and VOF method are used to capture the water free surface. And the motion of rigid body (as for ditching motion of aircraft) can be computed by using Dynamic Fluid Body Interaction (DFBI) method and Overset Mesh method. This paper predicts the violent skipping motions during ditching procedure of BWB-450 aircraft in calm, ignoring the influences from such facilities as engines, flaps, landing gears as well as winglets. And the wavy affects upon ditching behaviors are discussed basing on the numerical results. Owing to high horizontal speed at the beginning of ditching, the aircraft should travel a long distance. Although global mesh method(GMM) could be used to simulate the long-distance ditching process efficiently without occupying high computing resource, it losses the flexibility of calculation in multibody motions and has to reserve lots of extra fine grids to ensure accurate capture of the free liquid surface because of the rotation motion of aircraft. In particular, when the aircraft ditches on the water in a wavy environment, the motions of the computational domain boundaries will exert an influence in the accuracy of waveform for a long time. In response to the above problem, this paper tentatively proposes a satellite overset mesh scheme that combines the advantages of the global mesh method and overset mesh method, as shown in Figure 2.

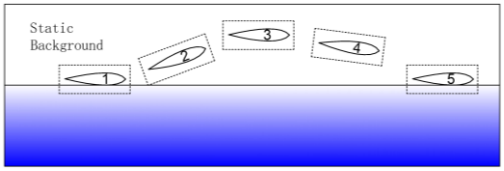

a) Dynamic overset region with static background region.

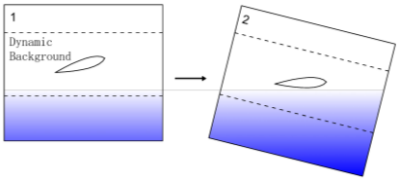

b) Global mesh method.

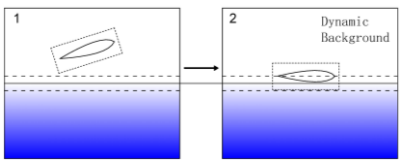

c) Satellite overset region with dynamic background region.

Figure 2 – Comparison with dynamic mesh methods.

2.1 Flow Solver

The finite volume method is used to discretized RANS equations and the pressure-velocity coupling is realized by a SIMPLE algorithm. The realizable k-ε model is selected as the turbulence model,

which can match the physical laws of real turbulence better than the standard k-ε model.

The VOF method is used to identify the free surface between air and water phases. The principle of VOF method is to define a function (such as water fraction function) which could describe the volume ratio (0~1) of the target medium (such as water) in a grid unit. When the volume fraction of the target fluid (such as water) is 1, it means that the medium in the grid is all water. While the volume fraction is 0, it means that there is no water in the grid cell. For the volume fraction of a grid unit between 0 and 1, it indicates that this grid unit is on the surface of water. In addition, the water-gas interface in the grid cell with a volume fraction between 0 and 1 is divided by methods such as distance function. In this way, the free surface between two fluid phases can be captured accurately.

2.2 Coupling of Wave Tank and Overset Mesh

Numerical wave tank refers to a computational domain built by numerical simulation methods for simulation of the interaction between wave water and moving objects. In this paper, the boundary method is used to make wave water, which updates the velocity, pressure, mass and the volume fraction at boundaries with time varying to realize numerical wave making. In addition, since the numerical wave tank is prone to wave reflections at the outlet boundary, measures need to be taken to avoid reflected waves.

By forcing Navier-Stokes equations towards a numerical solution on a simplified theory over some distance around the body, wave forcing[17] method can reduce the computing effort and eliminate reflected waves at the boundary. It is only suitable for the correction of the momentum source term. By adding the momentum source term to the momentum equation, the fluid momentum can be brought closer to the theoretical solution

$$q_{\phi} = -\gamma\rho(\phi - \phi^{*}). \tag{1}$$

where γ is the forcing coefficient,

ρ is the fluid density,

ϕ is the current solution of the transport equation,

ϕ^{*} is the value towards which the solution is forced.

The forcing coefficient is not constant in the forcing domain. Its strength decreases from the boundary to the Navier-Stokes equations solution domain, whose value is defined by formula (2)

$$\gamma = -\gamma_{0}\cos^{2}(\frac{\lambda}{2}x^{*}). \tag{2}$$

where λ is the wave forcing length.

As shown in Figure 3, overset mesh method generally requires a background region and several component regions for interpolation calculation, in which the priority of grids in overset region is higher than grids in background region. In interpolation calculation, the cells of low priority in overlapping region will be identified marked as the inactive by the hole-cutting process. And the active cells in the overset region and the background region will be coupled on the overlapping edge.

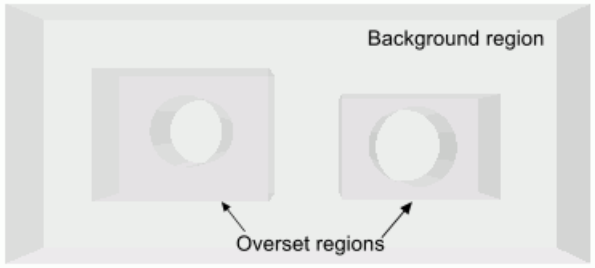

Figure 3 – Computational domain of overset mesh method.[17]

In this paper, the numerical scheme that couples overset mesh method and numerical wave tank

has been used to simulate the process of aircraft ditching. The wave tank is set as background region and the rigid body is set as overset region. Since the wave making and waveform maintenance of the numerical tank largely depend upon the grid, it is necessary to verify the accuracy of grid of wave tank under the influence of the overset region moving.

2.3 Coupling of Dynamic Rigid Body and Dynamic Computational Domain

In Star-CCM+ solver, the DFBI module is used to simulated the motion of a rigid body in response to pressure, shear force, volume force (such as gravity) as well as additional defined force. This paper uses the 6-DOF Dynamic Fluid Body Interaction method to calculated the acceleration and angular acceleration, which are integrated into velocity and angular velocity of moving body. The motion characteristics of the rigid body respond to the surrounding fluid by exerting force. In a time-step, the rigid body and the fluid flow respond to each other. The rigid body (BWB aircraft) and the overset region will move together while the background region will move at the same horizontal speed so that it can remains relatively stationary with the overset region in the horizontal direction, as shown in Figure 4.

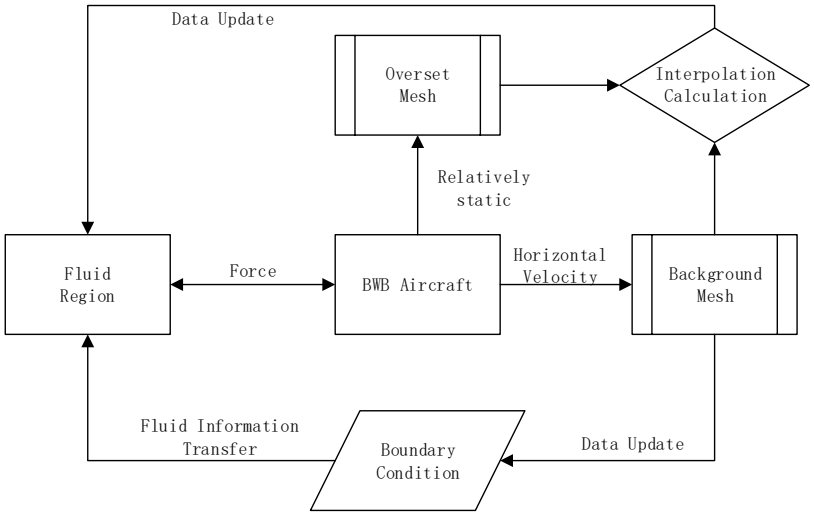

Figure 4 – Dynamic overset mesh process of ditching of BWB aircraft.

3. Validation of Numerical Method

3.1 Validation of Numerical Wave Tank

While investigating the influence of waves on the aircraft during ditching, the size of the BWB-450 model should be taken into account. The length of the fuselage is about 40 m and the wingspan is about 80 m. Therefore, the wave with the same wavelength as the length of fuselage is selected, which has a certain reference significance. In order to facilitate the description of the physical meanings of wave parameters, a schematic diagram of the wave is given in Figure 5. The wave chosen in this paper is the fifth-order Stokes wave, which is closer to the real water wave. The velocity of the wave is determined by the water depth (D), the wave height (H_w) and the flow velocity (U). The wave parameters are shown in Table 1.

Table 1 – Wave parameters.

Parameters	Values
Wave length	40 m
Wave height	2 m
Wave height/Wave length	0.05 (Linear wave)
Deep	100 m
Period of wave	5 s
Density of water	997.561 kg/m^3
Density of air	1.184 kg/m^3

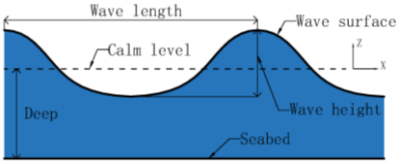

Figure 5 – Physical description of water wave.

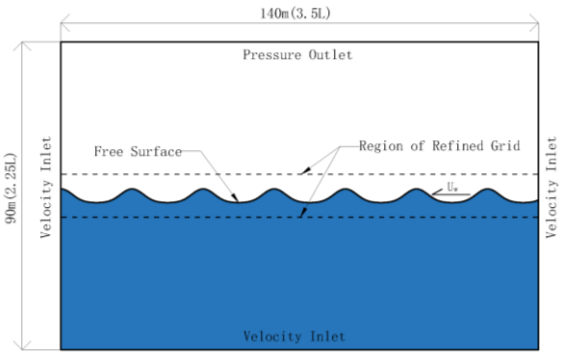

Figure 6 – Computational domain of static tank.

3.2 Static Wave Tank

The computational domain of the numerical wave tank chosen for Star-CCM+ is three dimensional. The domain is a length of 140 meters in x-direction (3.5 times the wave length), a height of 90 meters in z-direction and a thickness of 0.1 meters in y-direction that is only 0.25% of the wave length. The left, right and bottom boundaries are set as the velocity inlet, while the top boundary is the pressure outlet as shown in Figure 6. And the y-direction boundary plane is set as the symmetry plane. The grid is generated using Trimmer Mesh method in Star-CCM+ with the maximum cell size about 1.8 m not close to the wave surface. Grids near the free surface are refined, where the minimum cell size is about 0.45 m in x-direction and about 0.1 m in z-direction. The height of refined domain is 4 meters (2 times the wave height) and there is only one layer of grid in the y-direction, as shown in Figure 7.

In order to avoid the appearance of reflected wave, the correction of wave forcing method is added within one wave length distance (40 m) from left and right boundaries respectively. The time step is setup as 0.0005 s, and the realizable k-ε turbulence model is selected.

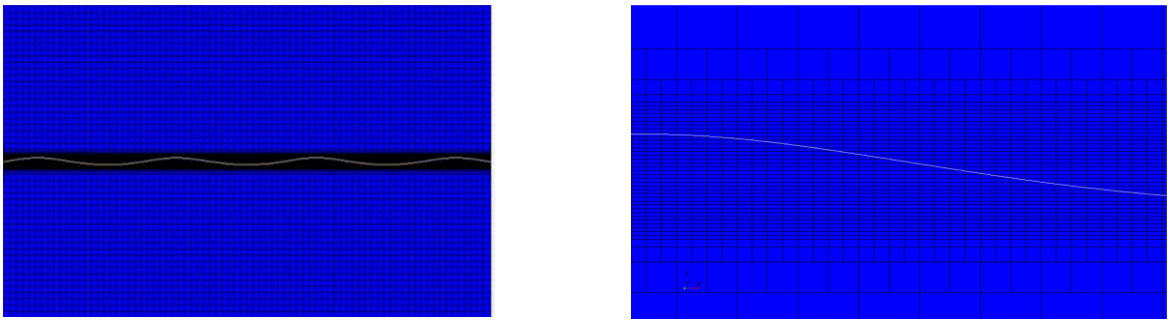

a) Global grid. b) Local grid in details.

Figure 7 – Grid of numerical wave tank.

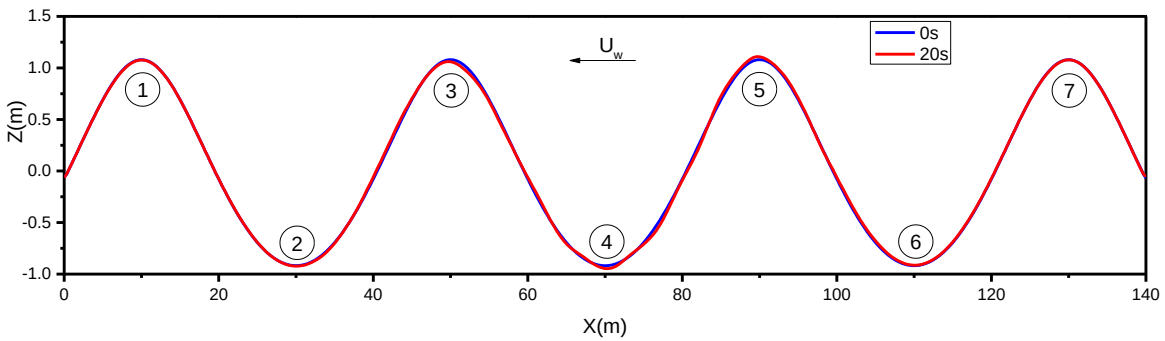

Figure 8 – Comparison of waveforms of 0 s and 20 s in static wave tank.

The results of waveforms during 20 s (4 periods) are obtained through calculation. Comparing the waveform results of 0 s and 20 s, the wave-making performance of numerical tank is verified, as

shown in Figure 8. And the values of the crests and the troughs in 0 s and 20 s are compared in Table 2. It can be seen that the waveform retention is acceptable after 20 s and the maximum attenuation of peak or trough is only about 3%. The velocity and pressure distribution of 0s and 20 s are shown in Figure 9 and Figure 10. Errors are defined as formula (3).

Table 2 Comparison of crests and troughs of 0 s and 20 s in static wave tank.

Crest or Trough	Value (0 s)	Value (20 s)	Errors
①	1.080m	1.077m	-0.277%
②	-0.918m	-0.923m	-0.545%
③	1.080m	1.060m	-1.85%
④	-0.918m	-0.947m	-3.16%
⑤	1.080m	1.110m,	2.78%
⑥	-0.918m	-0.914m	0.436%
⑦	1.080m	1.078m	-0.185%

$$Errors = \begin{cases} \dfrac{Crest(20s) - Crest(0s)}{Crest(0s)} \times 100\% \\ \dfrac{Trough(20s) - Trough(0s)}{Trough(0s)} \times 100\% \end{cases}. \tag{3}$$

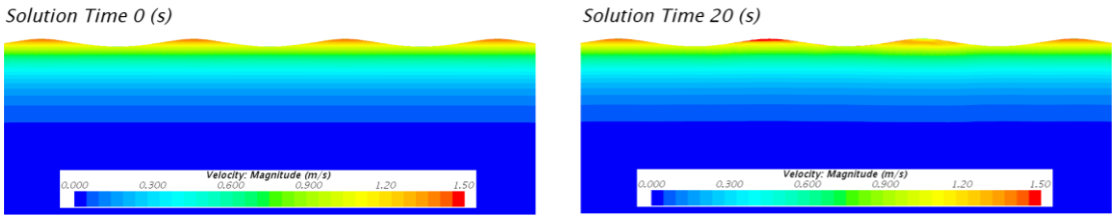

Figure 9 – Velocity distribution of 0 s and 20 s in static wave tank.

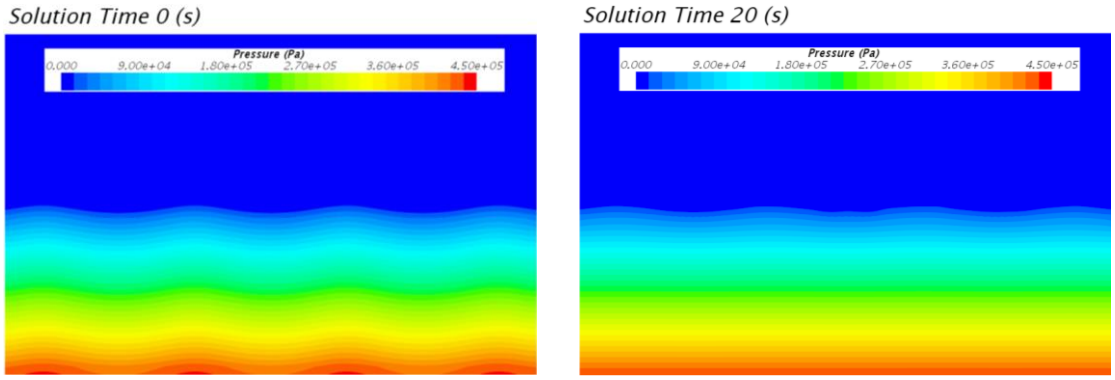

Figure 10 – Pressure distribution of 0 s and 20 s in static wave tank.

3.3 Dynamic Wave Tank.

The above has verified the wave-making accuracy and waveform retention capabilities of the numerical wave tank. Then, it is necessary to verify the interpolation calculation accuracy of overset mesh method, where the computational domain of static wave tank is set as the dynamic background region and a rectangular grid is set as the dynamic overset region. As shown in Figure 11, the motion of the overset region is defined by user-defined field function, in which the horizontal speed is constant (U=72 m/s) while the vertical speed (V) is defined as formula (4).

$$V = -5\sin\left(\frac{4\pi}{5}t + \pi\right). \tag{4}$$

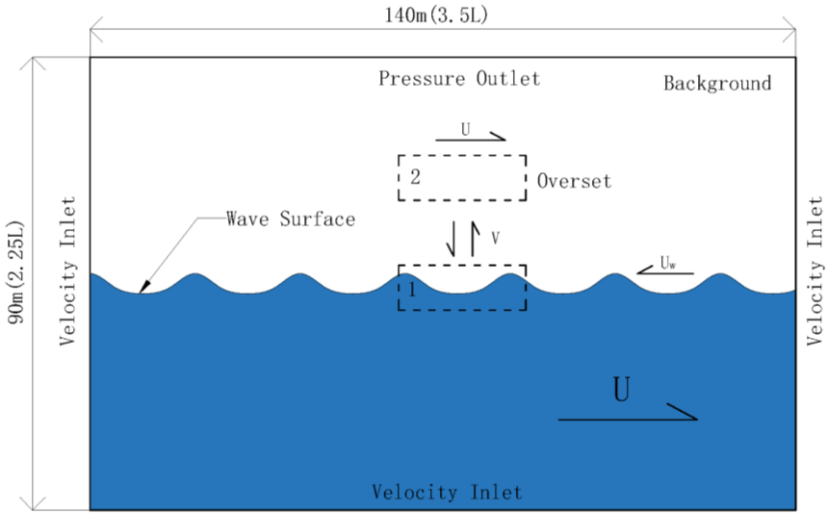

Figure 11 – Computational domain of dynamic wave tank.

Although the background region of dynamic wave tank is moving at the speed of 72 m/s in x-direction, the absolute speed of the wave (U_w=-8m /s) is same as the static wave tank. In order to compare the performances of static wave tank and dynamic wave tank, the encounter frequency of between wave and grid can be calculated by formula (5) and formula (6).

$$f_e = \frac{U_e}{\lambda}. \tag{5}$$

$$U_e = U - U_w. \tag{6}$$

where f_e is the encounter frequency;

U_w is the absolute speed of wave in x-direction;

U is the absolute speed of grid in x-direction;

U_e is the relative speed of the wave and the grid;

λ is the wave length.

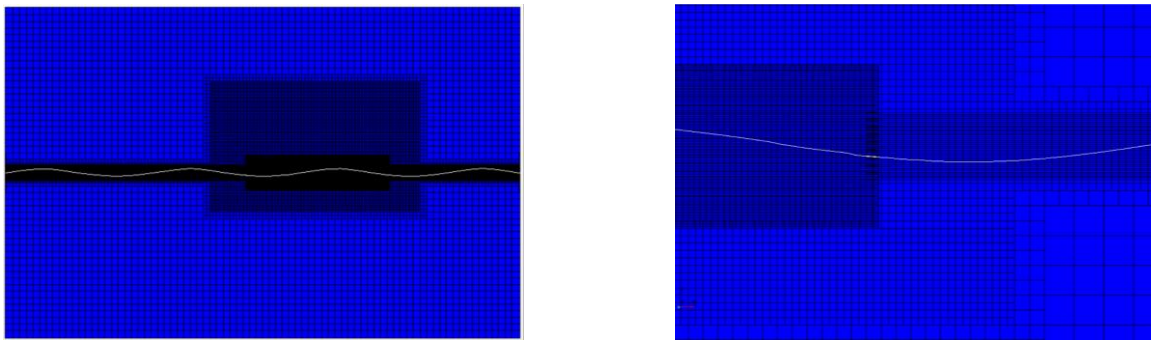

a) Global grid. b) Local grid in details.

Figure 12 – Grid of numerical wave tank using overset mesh method.

After calculating, the encounter frequency (f_e) of static tank is 0.2 s^{-1} and f_e of dynamic tank is 2 s^{-1}. It means that the encounter period of static tank is ten times longer than dynamic tank. In order to compare the waveforms of the same phase in the static tank and dynamic tank, the physical time of dynamic tank is one-tenth of static tank. Grid of dynamic wave tank is shown in Figure 12, and the waveforms in different time are compared in Figure 13. These results verify the accuracy of dynamic wave tank using overset mesh method, which lays the foundation for the numerical simulation of BWB-450 during ditching.

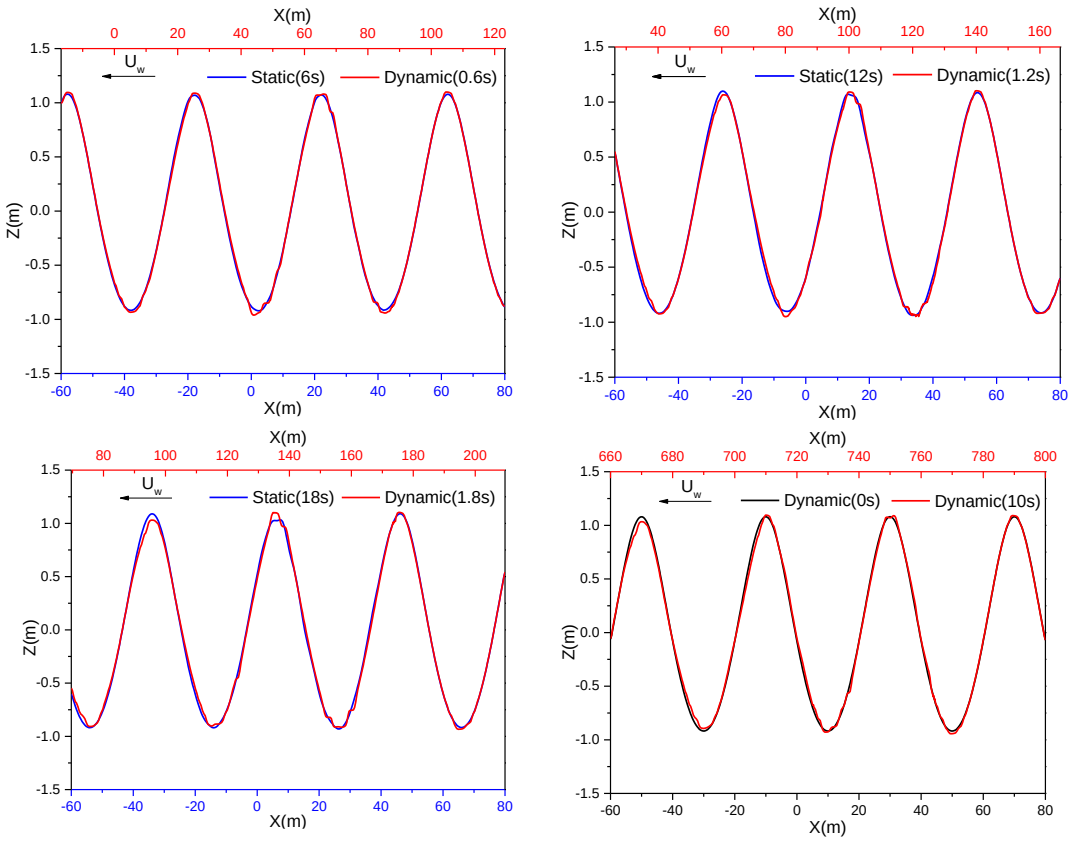

Figure 13 – Comparison of waveforms of static tank and dynamic tank in different time.

4. Ditching of BWB-450 Aircraft.

4.1 Physical Model and Computational Grid.

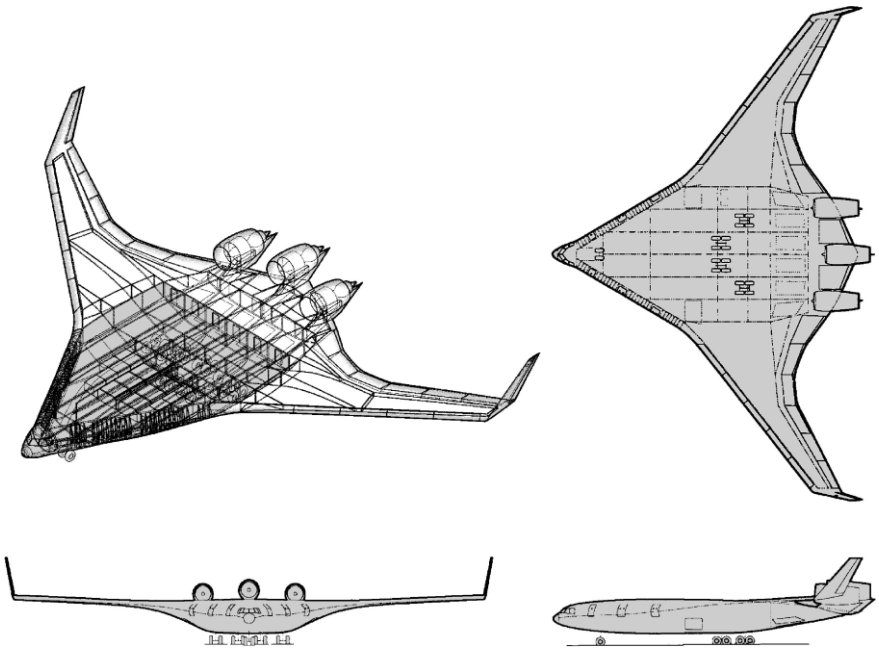

Figure 14 – Isometric view and three views of BWB-450 aircraft[4].

The calculation model selected in this paper refers to the Boeing BWB-450[4] blended wing body aircraft model of which the isometric view and three views is shown in Figure 14. Only symmetrical motions and loads are considered during ditching, therefore, the calculation model is a half geometry of BWB-450. Other geometric parameters are listed in Table 3, and the initial ditching parameters are given in Table 4.

Table 3 – Basic geometric parameters of BWB-450 aircraft.

Parameters	Values
Maximum Takeoff Weight (half)	218.5 t
Centre of Gravity	55% of the Longitudinal Axis
Length of Fuselage	40 m
Wingspan (half)	37.95 m
Reference Area (half)	325.7 m^2
Mean Aerodynamic Chord	9.965m
Initial Pitch Moment (half)	1.25×10^7 kg·m^2

Table 4 – Initial ditching parameters of BWB-450 aircraft.

Parameters	Values
Initial Pitch Angle	12 °
Initial Horizontal Speed	72 m/s
Initial Vertical Speed	-1.5 m/s

On the one hand, the influence of the wingtips is not significant during the ditching. On the other hand, the overset mesh method has the high requirement for the uniformity of overset grid around the aircraft, while the existence of wingtips is not conducive to maintain the good transition between overset grid and background grid. Consequently, the simplified clean configuration of BWB-450 aircraft without winglets is chosen as the calculated model in this paper, whose half model is shown in Figure 15. In order to improve the grid quality of fuselage surface, a structural grid of overset region is adopted. And the background grid of the numerical wave tank is generated by trimmer mesh method, which has acquired the numerical accuracy in validation of numerical wave tank. The computational domain with boundary conditions has been shown in Figure 16.

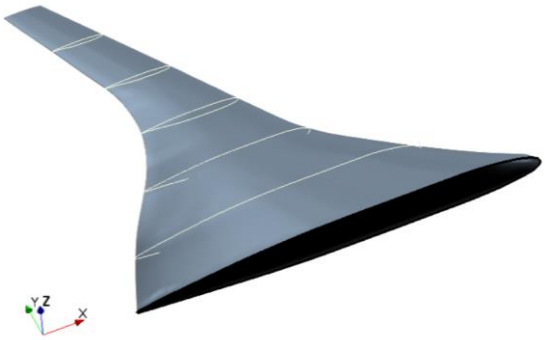

Figure 15 – Simplified half model of BWB-450 aircraft.

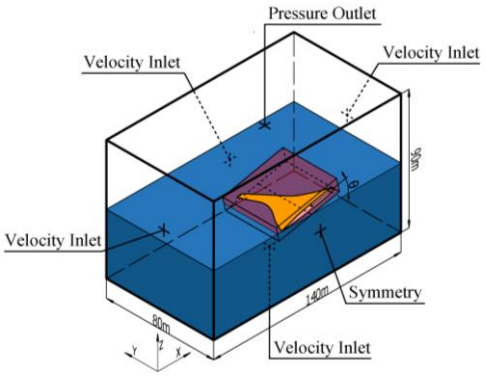

Figure 16 – Computational domain of BWB-450 aircraft.

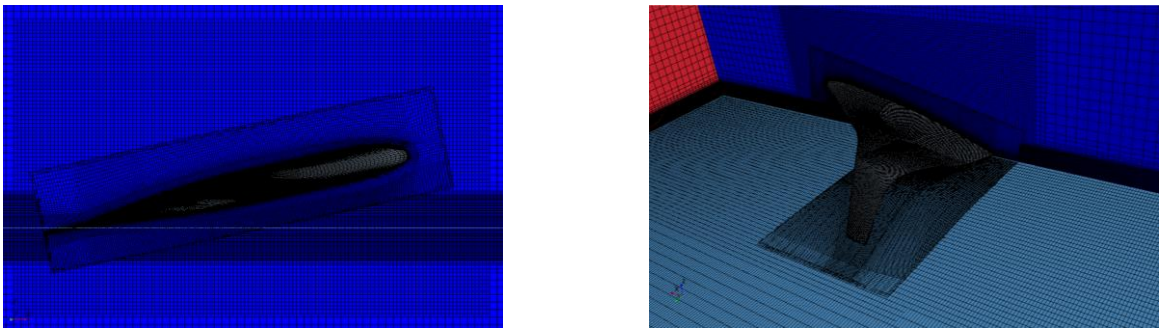

Figure 17 – Local grid of BWB-450 aircraft in details.

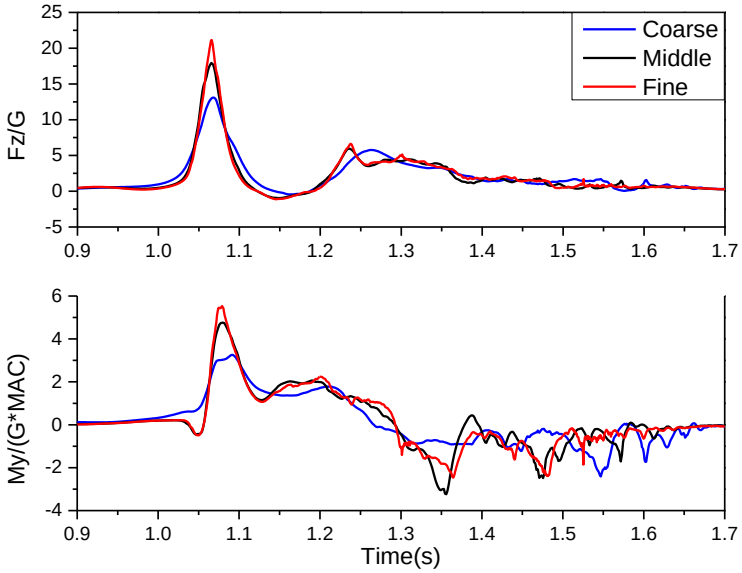

Figure 18 – Grid independence verification of BWB-450 aircraft during ditching.

The vertical load and pitch moment in the coarse (about 0.5 million), middle (about 4 million) and fine (about 6.7 million) grid of BWB-450 aircraft during ditch on calm water are compared in Figure 18. Considering to keep the balance of computing accuracy as well as simulating efficiency, the middle grid is selected in the subsequent simulation of ditching on calm water and wavy water.

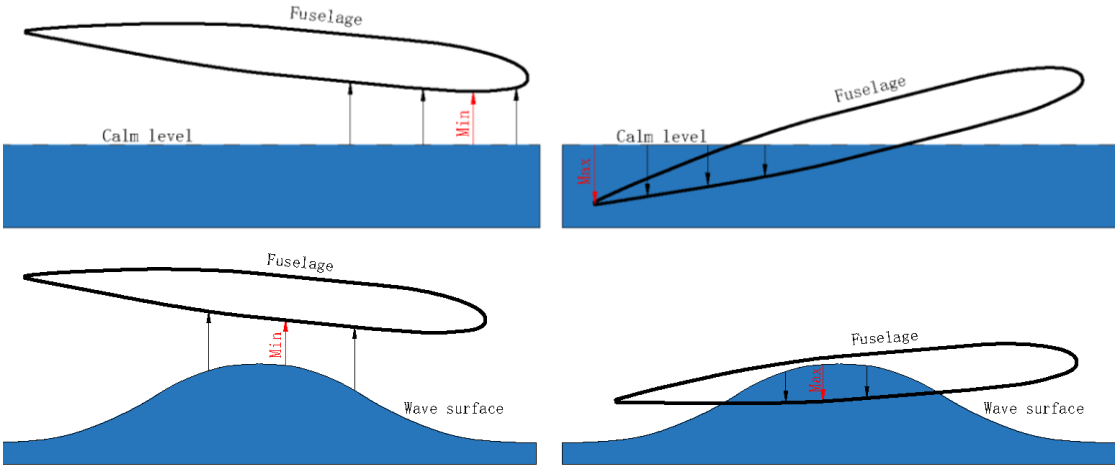

Figure 19 – Deepest point of fuselage during ditching on calm water and wavy water.

For describing the relative position between fuselage and water surface, the deepest point on the symmetry plane of BWB-450 aircraft fuselage is defined as shown in Figure 19. When the aircraft is completely out of water, the deepest point refers to the closest point of fuselage to the water surface. While part of fuselage is in the water, the deepest point means the maximum distance of fuselage below water free surface. It means that the deepest point is negative when part of the fuselage contacts the water, and the positive value of the deepest point refers to the aircraft completely in air.

4.2 Skipping on Calm Water.

After simulating for a long time, the motion characteristics of BWB-450 aircraft during three periods of skipping are exhibited in Figure 20. A period of skipping motion is defined that it begins when the value of deepest point changes from positive to negative, until the next period begins. The pitch attitude of BWB-450 aircraft varies, and the change of heaving lags behind the pitching. As shown in Figure 21, when the fuselage starts to get into the water (the deepest point becoming smaller than value of water level), the vertical load rises sharply.

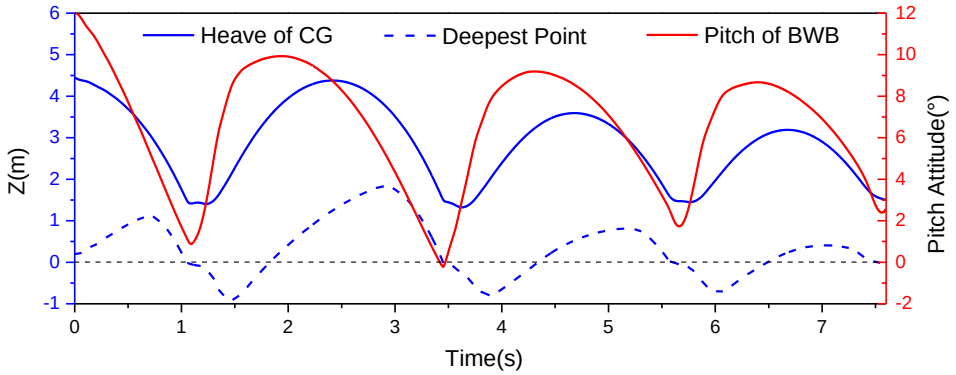

Figure 20 – Motion changes of BWB-450 aircraft during ditching on calm water.
(Heave of CG——Vertical positon change of center of gravity.
Lowest Point——Vertical positon change of lowest point of fuselage
Pitch of BWB——Pitch attitude change of fuselage.)

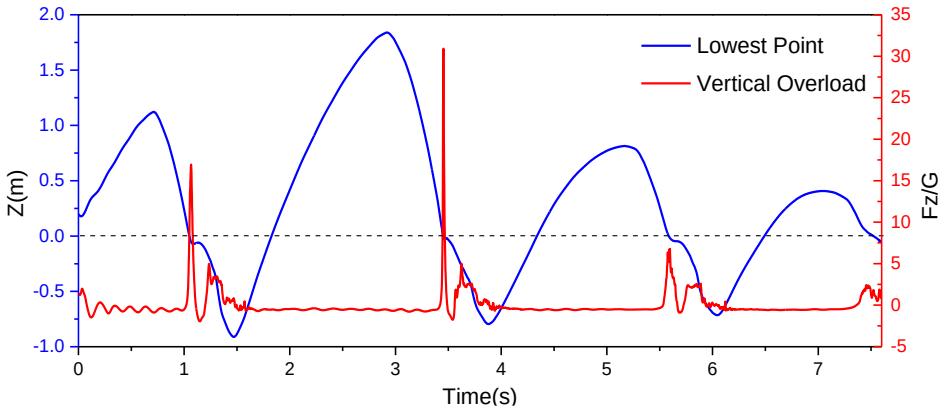

Figure 21 – Vertical overload changes of BWB-450 aircraft during ditching on calm water.

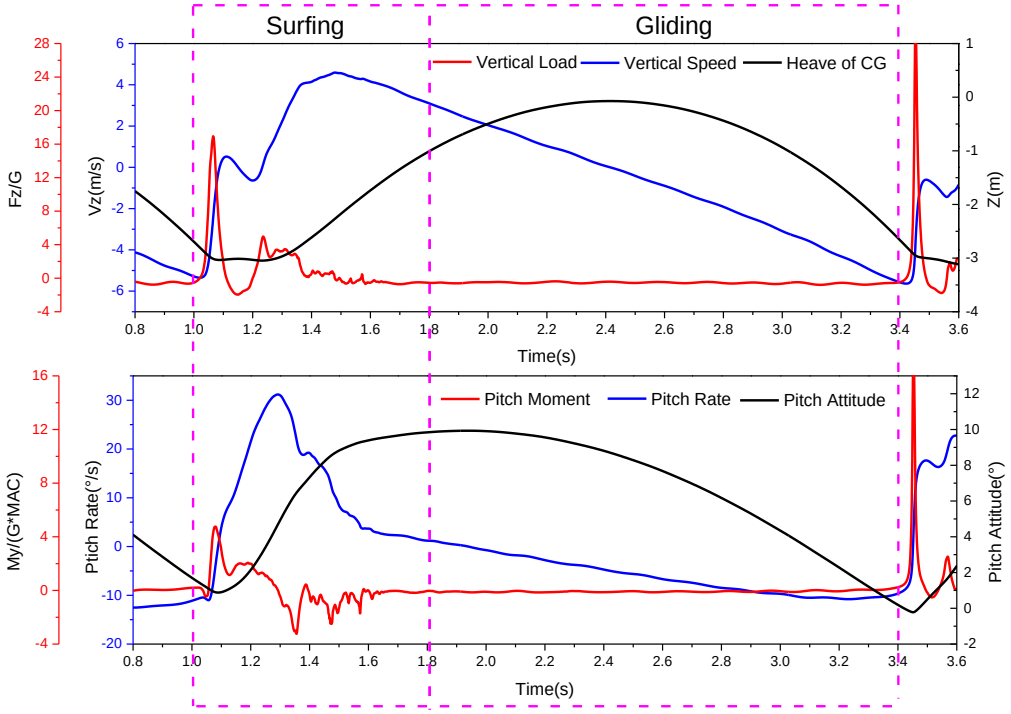

Figure 22 – A period of skipping during ditching on calm water.

According to the attitude of BWB-450 aircraft and the load characteristic, one period is divided in two stages, in which the deepest point is negative in the first stage defined as surfing and keeps greater than zero (the calm water level) during the second stage defined as gliding. Thus, a period of skipping

during ditching from 1 s to 3.4 s is analyzed below in detail, as shown in Figure 22.

4.2.1 Surfing Stage

In this period, the length of the gliding stage is about twice the length of the surfing stage. At the beginning of the surfing stage, the aircraft collided with water violently at a low attitude when the “potted” high-pressure area appears on the belly of the fuselage. And then a hydrodynamic high-pressure zone of strip shape is developed on the bottom surface of the aircraft. After the primary water impact on the bottom of the fuselage, the aircraft begins to nose up for the nose-up moment coming from the positive pressure ahead of the center of gravity as well as the negative pressure behind of the center of gravity. The changes of the attitude and the relative position are shown in Figure 23 a) and Figure 23 b) separately. And the typical pressure distributions are shown in Figure 23 c).

As the attitude gets higher, the pitch rate reduces gradually while the pitch angle of the fuselage rises to the top as shown in Figure 22. The high attitude of the aircraft causing by the nose-up moment converts some draft into lift, which raises the aircraft to skipping. With the attitude and the vertical position of aircraft higher, the vertical hydrodynamic load decreases, and the wetted area recedes from the rear on the bottom surface as shown in Figure 23 c).

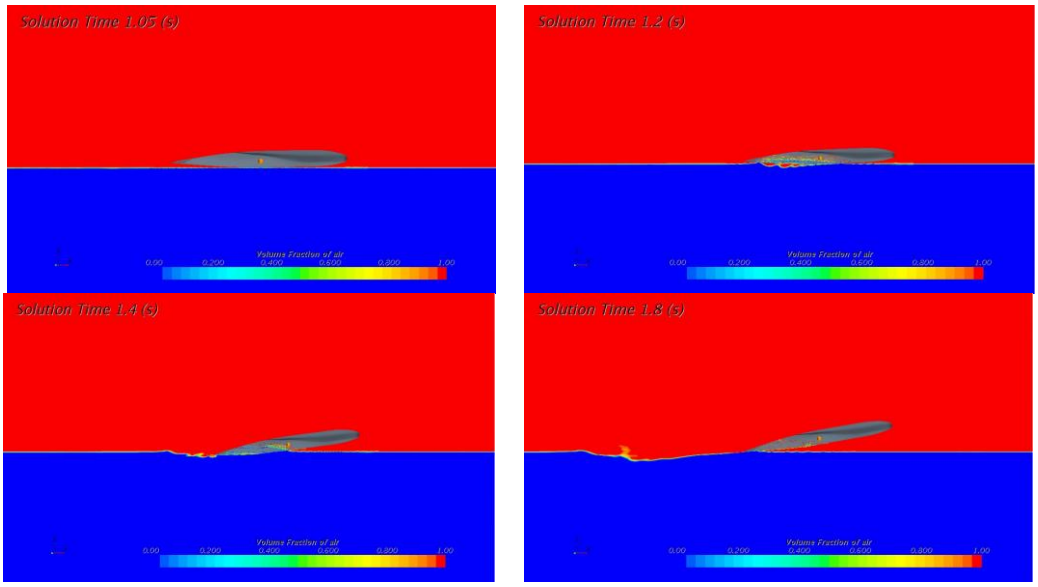

a) Change of the attitude in the surfing stage.

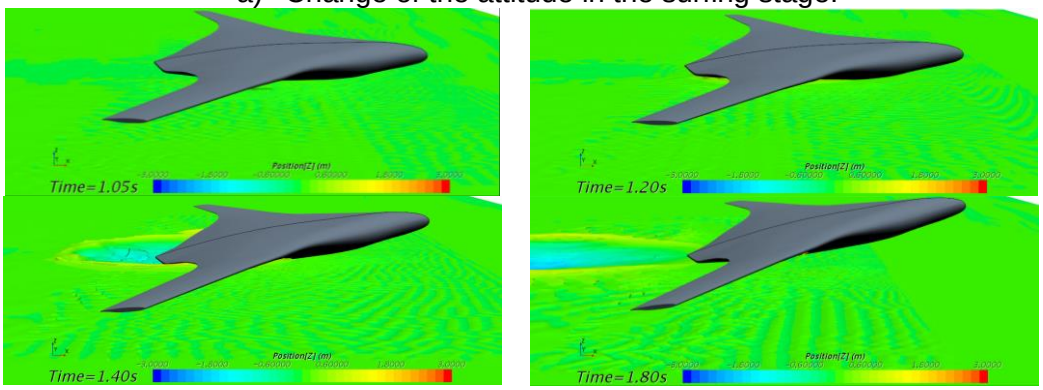

b) Change of the water surface in the surfing stage.

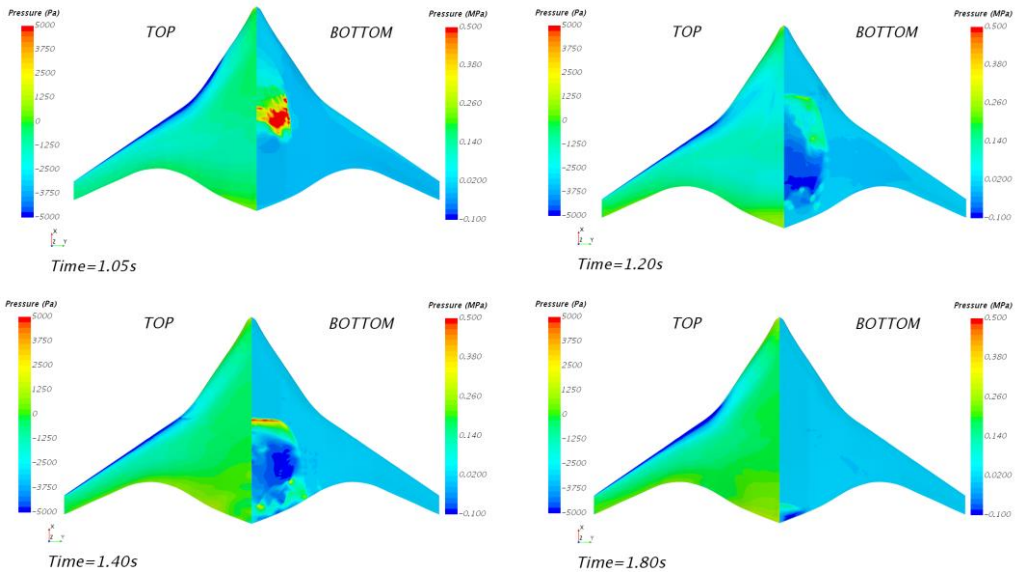

c) Pressure distributions in the surfing stage.

Figure 23 – Typical moments of BWB-450 aircraft during ditching in the surfing stage.

Besides the great hydrodynamic impact on the fuselage, however, a suction area occurs on the bottom the tail caused by the Coanda effect. For analyzing the effect of the suction area upon the plummet of the vertical load and the nose-up behavior at a low attitude (around 1.15 s in Figure 22), the pressure distribution and the surface curvature of the bottom are exhibited below. In Figure 24, the area at the tail with the denser contours indicates the greater surface curvature where the suction pressure can be seen. The profile curves of the fuselage in section A and section B are shown in Figure 25. Therefore, the large curvature of the tail results in the Coanda effect, which reduces the vertical load on the one hand, and also makes the aircraft nose up quickly (around 1.15 s), as shown in Figure 22.

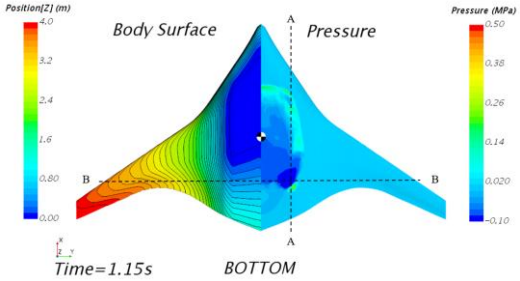

Figure 24 – Curved surface shape and pressure distribution on the bottom of the fuselage.

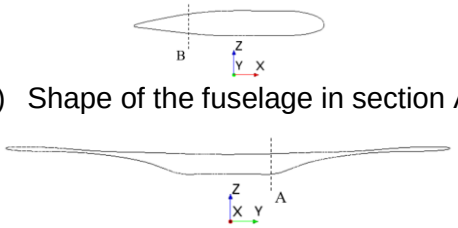

a) Shape of the fuselage in section A.

b) Shape of the fuselage in section B.

Figure 25 – Body Section Shape of BWB-450 aircraft.

4.2.2 Gliding Stage

During the stage of gliding, the aircraft jumps out of the water with the large pitch angle and the behavior resembles the oblique throwing motion. The attitude changes as shown in Figure 26.

Comparing with the stage of surfing in Figure 22, the aircraft in the gliding stage endures relative smaller load, of which the pitch rate and the attitude reduces gradually until the next impact on the water. Meanwhile, it can be seen in Figure 22 that the pitch moment of the aircraft is negative (nose-down) during gliding, and the pitch rate of the aircraft decreases from around 0 °/s to -10 °/s gradually. Since the aircraft has been completely out of the water, the nose-down moment should come from aerodynamics.

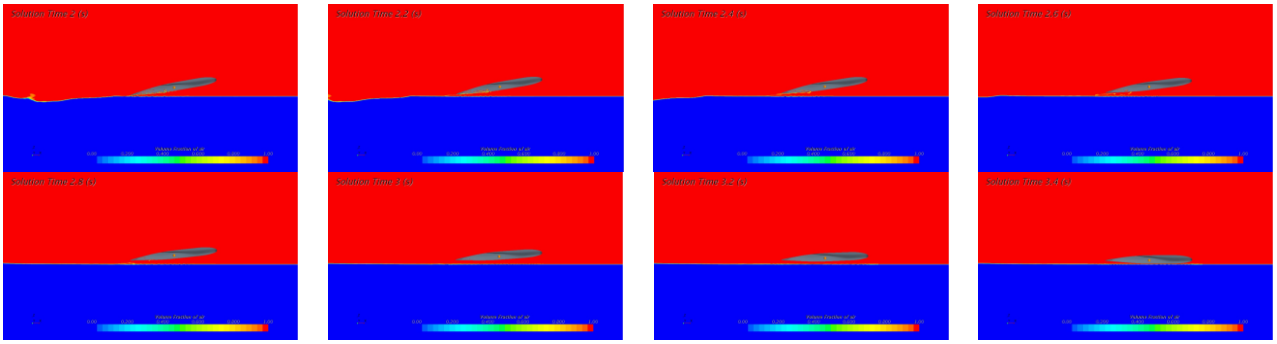

Figure 26 – Change of attitude of BWB-450 aircraft during gliding.

4.3 Skipping on Regular Waves.

The process of ditching on wavy environment is investigated in this paper. As shown in Figure 27, the propagation direction of the waves is opposite towards the horizontal speed of the aircraft. In the initial calculation, the real edge is located at the trough, where the aircraft endures the largest loads at the first impact. Parameters of the wave are exhibited in Table 1. Other parameters of the initial attitude as well as the initial speed are the same as those for ditching on calm water.

The different results between on calm water and on wavy water are compared and analyzed as follows. As shown in Figure 28, the aircraft also behaves the skipping motion during ditching on wave water. However, the periodicity of the aircraft in wavy environment is partially affected by waves compared with on calm water, which displays the swifter horizontal deceleration and the greater moving amplitude.

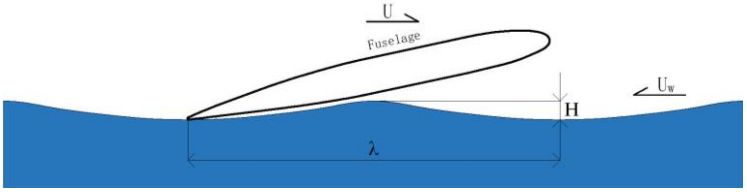

Figure 27 – Description of the relative position between the aircraft and the waves.

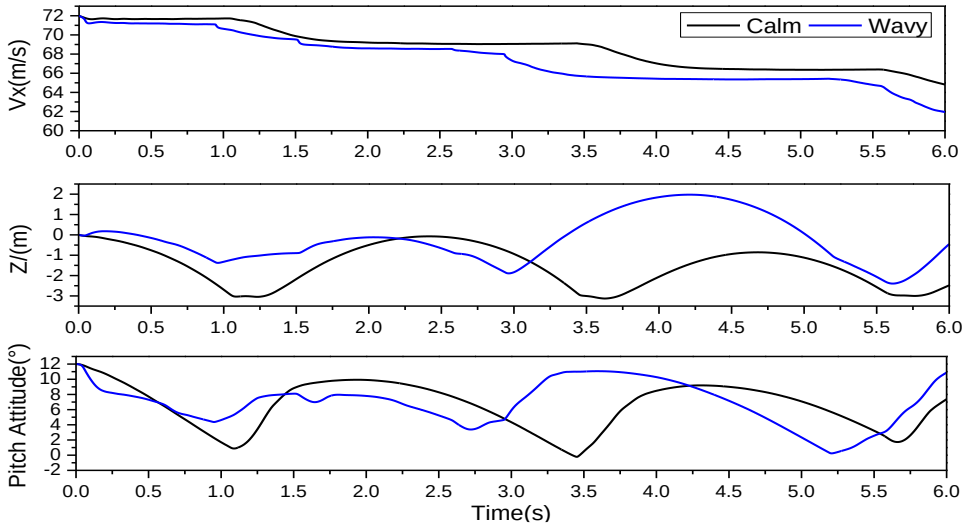

Figure 28 – Comparison of BWB-450 aircraft during skipping on calm water and wavy water.

The attitudes and the distributions of BWB-450 aircraft during ditching at typical moments in wavy environment are shown in Figure 29. The attitude at 0.1 s represents the rear of the aircraft impacting on the water, and the moment of 5.7 s exhibits the green water hits on the head of the aircraft, in which part of the water splashes and flows over the upper surface of the fuselage. It can be analyzed

that during only the rear of the fuselage touching water, the hydrodynamic load on the aircraft is lower and a larger nose-down moment is generated. While the head of the fuselage is impacting on the wave surface, the wetted area spreads to nearly whole bottom of the aircraft. And then, a large suction zone occurs on the front part of the fuselage with the high water impact. To contrast with the calm water, the probability of the aircraft's head hitting the water surface (green water) in a wavy environment is greatly increased.

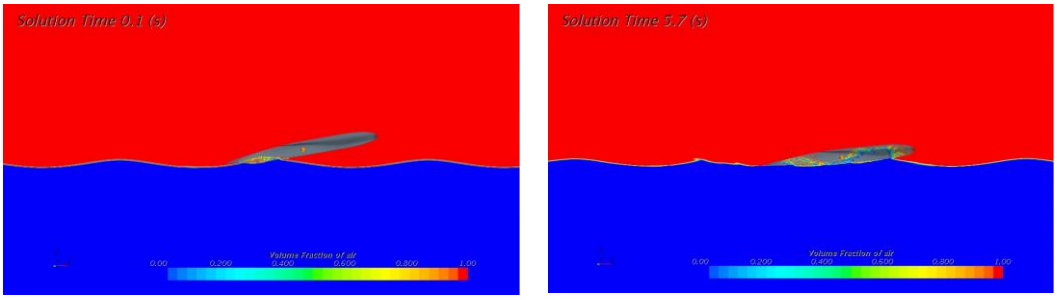

a) Typical attitudes of BWB-450 aircraft.

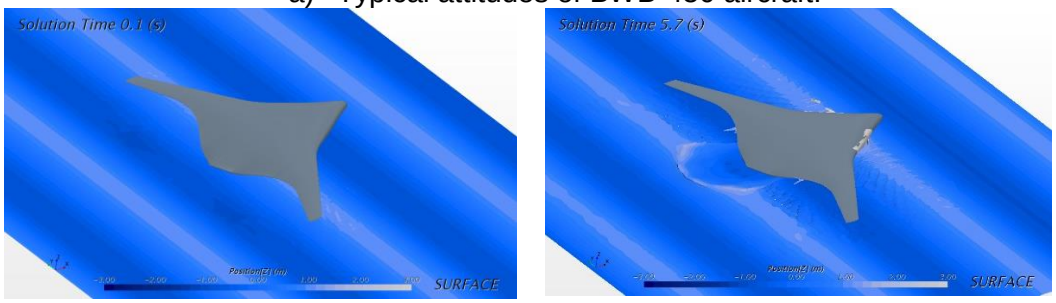

b) Typical positions of BWB-450 aircraft.

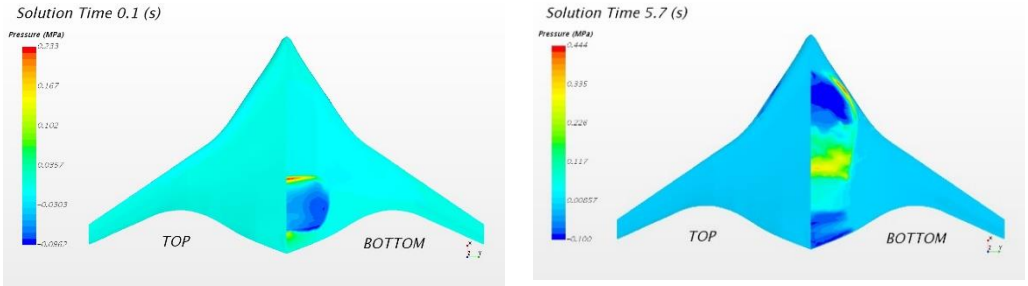

c) Typical pressure distributions of BWB-450 aircraft.

Figure 29 – Typical moments during ditching in wavy environment.

If the aircraft keeps contacting with water like porpoising, increasing the wave length and decreasing the horizontal speed will both reduce the encounter frequency, which play the same effect on the ditching behavior. Nevertheless, the phenomenon of the aircraft skipping over waves appears during ditching in the wavy environment, as a result of which the motion of aircraft is not always affected by waves. It means that increasing the wave length and decreasing the horizontal speed fails to obtain the similar response. This phenomenon tends to occur after the aircraft's head hits on the wavy surface.

As shown in Figure 30, wave level of center of gravity (CG) represents the vertical position of the wave surface when the aircraft's center of gravity moves to the same position in x-direction. When the deepest point is higher than the wave level, the motion of the aircraft is not affected by hydrodynamics that belongs to the stage of gliding. At this time, the horizontal speed of the aircraft remains general constant. When the deepest point is lower than the wave level, the movement of the aircraft is affected by the fluctuation of the wavy surface and the horizontal speed is greatly reduced, which belongs to the stage of surfing.

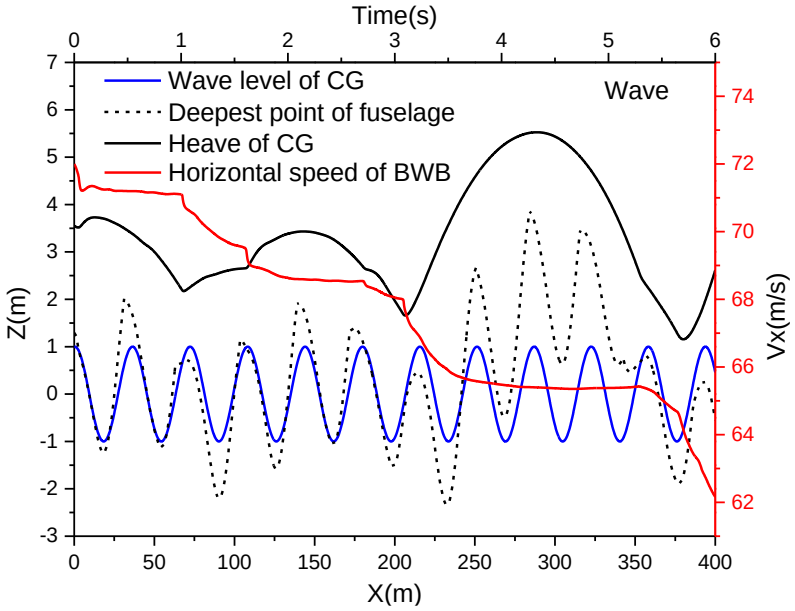

Figure 30 – Motion changes of BWB-450 aircraft during ditching in wavy environment.

When the aircraft experiences the skipping motion in the early stage of ditching, whether on calm water or wavy water, the aircraft's horizontal speed presents a series of stepwise decreases. Because the influence on aircraft's motions is exerted by wave surface only in the stage of surfing and the horizontal speed of aircraft is generally unchanging in the gliding stage. Therefore, the BWB aircraft will maintain skipping with high horizontal speed for a long time until the velocity failing to support to rebound from water.

5. Conclusion

In this paper, numerical method of FVM is selected to investigate the behavior characteristics of BWB-450 aircraft during ditching on calm water as well as in wavy environment. And the feasibility of dynamic overset mesh method in simulating the ditching procedure is explored.

The numerical simulation results show that while ditching at a high horizontal speed the blended wing body aircraft will experience the continuous skipping motions. This dangerous phenomenon not only increase the distance of ditching, but makes the aircraft endure severe hydrodynamic load many times. The results of BWB-450 aircraft during ditching on regular waves indicate that the wave environment amplifies the uncertainty and risk of the aircraft entering water in the skipping process. Meanwhile, a typical wavy environment with the wave length of 40 m and the wave height of 2 m affects the ditching performance of aircraft, which makes the aircraft more prone to skip and decelerate more rapidly.

Compared with the traditional aircraft, the shape of the fuselage of blended wing body aircraft makes it face greater danger during ditching. Therefore, more adequate considerations should be taken in the structure design and verification process for blended wing body aircrafts.

6. Contact Author E-mail Address

Corresponding author at: School of Aeronautical Science and Engineering, Beihang University, Beijing 100191, People's Republic of China

Peiqing Liu: lpq@buaa.edu.cn

7. Copyright Statement

References

[1] О.П. Шорыгин, А.Н. Беляевский, and Л.Г. Гонцова, "Моделирование вынужденной лосадки авиационно-космической техники на воду[A]," in ЦАГИ 90-лемия юбилейный сборник[C], Москва, 12.2008, pp. 100-107.

[2] National Transportation Safety Board, "Loss of Thrust in Both Engines After Encountering a Flock if Brid and Subsequent Ditching on the Hudson River, US Airway Flight 1549, Airbus A320-214, N106US Weehawken, New Jersey January 15, 2009[R]," Aircraft Accident Report NTSB/AAR-10/03, PB2010-910403,2010.

[3] P. Okonkwo, and H. Smith, "Review of evolving trends in blended wing body aircraft design," 2016, Vol. 82, pp. 1-23.

[4] R. H. Liebeck "Design of the Blended Wing Body Subsonic Transport," Journal of Aircraft, Vol. 41, No. 1, 2004, pp. 10-25.
doi: 10.2514/1.9084

[5] James Hileman, Zoltan Spakovszky, Mark Drela and Matthew Sargeant, "Airframe Design for "Silent Aircraft"[R]," AIAA-2007-453,2007.
doi: 10.2514/6.2007-453

[6] Lloyd J. Fisher, "Ditching Tests of A 1/20 Scale Model of the Northrop B-35 Airplane[R]," NACA Report SL8A29, 1948.

[7] D. Stinton, "Aero-marine Design and Flying Qualities of Floatplanes and Flying-boats[J]," Aeronautical Journal, Paper No. 1498, 1987, pp. 119.

[8] A.G. Smith, C.H.E. Warren, and D.F. Wright, "Investigations of the Behaviour of Aircraft When Making a Forced Landing on Water (Ditching)[R]," Aeronautical Research Council, Reports and Memoranda No.2917,1957.

[9] Lloyd J. Fisher and John O. Windham, "Ditching Investigate of A 1/11-Scale Model of the Chance Vought F7U-3 Airplane[R]", NACA Report SL52K07a, 1958.

[10] John B. Parkinson, "Notes on the Skipping of Seaplanes[R]", NACA Wartime Report, RB No. 3127, 1943.

[11] Lloyd J. Fisher and Edward L. Hoffman, "Ditching Investigations of Dynamic Models and Effects of Design Parameters on Ditching Characteristics[R]," NACA Report 1347,1958.

[12] H. Streckwall, O. Lindenau, and L. Bensch, "Aircraft Ditching: A Free Surface/Free Motion Problem[J]," Archives of Civil and Mechanical Engineering, vol. 7(3), 2007, pp. 177-190.
doi:10.1016/S1644-9665(12)60025-9

[13] Qu, Q., Hu, M., Guo, H., Liu, P., and Agarwal, R. K. "Study of Ditching Characteristics of Transport Aircraft by Global Moving Mesh Method," Journal of Aircraft, vol. 52, No. 5, 2015, pp. 1550-1558.

[14] R. Sturm, M. Hepperle, "Crshworthness and Ditching Behavior of Blended Wing Body (BWB) Aircraft Design[A]," German Aerospace Center (DLR), German, 2017.

[15] Zhirong Shen, Yi-Fang Hsieh, Zhongfu Ge, Richard Korpus, and James Huan, American Bureau of Shipping, "Slamming Load Prediction Using Overset CFD Methods[A]," Offshore Technology Conference[C], Houston, 2-5 May 2016.

[16] Dominic D.J. Chandar, and Venkata B L Boppana, "A Comparative Study of Different Overset Grid Solvers Between OpenFOAM, STAR-CCM+ and ANSYS-Fluent[A]," AIAA Aerospace Science Meeting[C], AIAA SciTech Forum, Kissimmee, Florida, USA, 8-12 January.
doi:10.2514/6.2018-1564

[17] Star-CCM+12.0 UserGuide, pp. 4315-4316.

[18] Lintang Chu, “Seaplane Hydrodynamic Design[M]”, Aviation Industry Press, 2014, pp.92-94 (in Chinese).